Structure and magnetism of self-assembled Fe nanowires on a faceted Cu(332) surface: the influence of oxygen-induced reconstruction

Structure and magnetism of self-assembled Fe nanowires on a faceted Cu(332) surface: the influence of oxygen-induced reconstruction

Carlos Eduardo ViolBarbosa[1]**, Jun Fujii**[1]**,
Giancarlo Panaccione**[1,3] **and Giorgio Rossi**[1,2]

[1] TASC Laboratory INFM-CNR, S.S. 14—km 163.5 in AREA Science Park,
I-34012 Basovizza (Trieste), Italy
[2] Dipartimento di Fisica, Università di Modena e Reggio Emilia,
via Campi 213/A, I-41100 Modena, Italy
E-mail: giancarlo.panaccione@elettra.trieste.it

Abstract. We present a study on the structural and magnetic properties of Fe nanowires as grown on an oxidized-reconstructed Cu(332) surface. A template surface consisting of alternate parallel stripes of Cu(111) terraces and (110) oxidized facets, with a periodicity of 4 nm, was used to grow iron wires, by the selective affinity of iron to the oxygen adsorption sites. Atomic resolution scanning tunnelling microscopy shows that Fe grows preferentially on the (110) facets, forming well-ordered Fe nanowires in the submonolayer regime. The (111) terraces are not affected by the iron deposition. Magneto-optical Kerr effect and x-ray magnetic circular dichroism reveal a long-range magnetic ordering of the wires with an out-of-plane magnetic easy axis at an early stage of the Fe growth. For coverages higher than 2–3 atomic layers, the magnetization switches to in-plane, but is perpendicular to the stripes.

[3] Author to whom any correspondence should be addressed.

Contents

1. Introduction

Manipulating surface/adsorbate systems with the aim of guiding the assembly of atomic and molecular organized structures is expected to lead to efficient ways of parallel 'bottom-up' fabrication of nanoscale functional patterns. Growth phenomena at surfaces are intrinsically 'template' i.e. chemically and kinetically driven by the surface topography and electronic structure. The 'mesoscale forces', corresponding to stress/strain fields, structural anisotropies and local coordination sites, that are present at reconstructed substrate surfaces, steer the growth of metallic overlayers and, in the case of iron, may lead to the formation of nanowires [1, 2].

Phenomenologically, it turns out that the mesoscale forces can be represented in terms of the anisotropic diffusivity D of the iron atoms at the surface. Templated growth is governed by kinetic effects; hence, the ratio between D and the deposition rate, F, has been used to describe the nucleation and growth of nanostructures at surfaces [2]. Typically, nanowire formation is obtained at low temperatures, i.e. by controlling D, which is the deposition rate determined by source and ultra-high vacuum (UHV) constraints. The ordering of Co nanodots on Au(788) (surface periodicity close to 3.9 nm) has been studied versus surface temperature by Rohart *et al* [3], who observed optimal alignment of Co nanodots on Au(788) at temperatures between 65 and 170 K. For Pt(997) with a surface periodicity of 2.0 nm, monoatomic rows of Co have been synthetized only in the temperature interval between 250 and 300 K [5]–[7]. Cu has been used as a template in several systems [8]–[13], including Fe–Cu. Guo *et al* [8] reported the formation of monoatomic Fe rows with a periodicity of 3 nm on a vicinal Cu(111), with the substrate kept at 120 K. Isolated Fe wires were grown on a vicinal Cu(111) with a 10 nm step size, and with the substrate kept at 0 °C ([9] and references therein). The iron/copper system has an attractive special feature: the close match between the lattice constant of the fcc copper ($a_0 = 3.61$ Å) and the one of the metastable fcc phase of iron (γ-Fe, $a_0 = 3.59$ Å) has led to the interpretation of the early stages of the epitaxial growth as γ-Fe, which displays a complex magnetic phase diagram and a strong spin–lattice coupling [9, 14, 15]. This conclusion has been challenged by Varga and co-workers [16], who rather favour a distorted bcc structure that relaxes as the thickness grows. A reorientation transition of the magnetization, from perpendicular to in-plane, has been observed in Fe/Cu(111) two-dimensional layers, accompanied by a Fe structural transition from the pseudomorphic distorted fcc phase to the bcc phase [9].

The design of different nanostructured magnetic systems is important for the study of the order–disorder magnetic phenomena. Concerning the unidimensional systems, it was demonstrated that the long-range magnetic order behaviour of a metastable character exists in the one-dimensional (1D) atomic Co chains deposited on Pt [17]; this phenomenon is ascribed to a strong magnetic anisotropy [17, 18]. Unstable magnetization was also observed in iron nanowires on vicinal copper [9].

IOP Institute of Physics Φ DEUTSCHE PHYSIKALISCHE GESELLSCHAFT

In the present paper, we analyse the results of the template growth of submonolayer amounts of iron deposited onto an optimally oxidized Cu(332) surface that presents alternate parallel stripes of pure Cu(111) and oxidized Cu(110) facets. Exposure of vicinal Cu(n, n, $n-1$) surfaces to oxygen induces a reconstruction consisting of alternating Cu(111) and Cu(110)O(2×1) facets (stripes) [19], as revealed by scanning tunnelling microscopy (STM). The presence of oxygen is confined to the (110) stripes. The (111) facets are undistinguishable from the ideal Cu(111), except for quantum confining effects perpendicular to the stripes [20]. Exploiting the higher affinity of iron with the oxidized stripes compared to pure copper, we obtain the self-organized growth of iron nanowires for a broad range of deposition conditions (thickness, temperature, deposition rate). The *in situ* analysis of the Fe magnetic properties, by means of the vectorial Kerr effect and by synchrotron-polarized x-radiation spectroscopy and magnetometry (x-ray absorption/x-ray magnetic circular dichroism XAS/XMCD), reveals that the magnetization of the ultrathin wires is oriented out-of-plane at the early stage of growth. The magnetization switches to in-plane, perpendicular to the stripe axis, for thicknesses >2.3 ML.

2. Experimental methods

The Cu(332) surface is vicinal to Cu(111), with a nominal miscut of $10°$. The terraces consist of 5 1/3 atomic rows ($l = 12\,\text{Å}$), as confirmed by the STM measurement. The clean surface was obtained in ultra-high vacuum (UHV) ($P < 1 \times 10^{-10}$ mbar) by repeated cycles of 650 eV accelerated Ar^+-ion sputtering and annealing at $500\,°C$, followed by slow cooling to room temperature (RT). The surface composition and long-range order were routinely probed by Auger electron spectroscopy (AES) and low-energy electron diffraction (LEED). The Cu(332) surface was oxidized by exposure to a 99.998% pure oxygen pressure of 5×10^{-8} mbar followed by 10 min annealing at $100\,°C$. Figure 1 shows the O–Cu(332) with (110) and (111) facets, as measured *in situ* by STM. It is important to underline that the stripe periodicity can be tailored by controlling the oxidation process of the Cu pristine (332) surface [21]. Average periodicities from 3 to 10 nm have been reproducibly obtained. Here we show the results of iron deposition on a template with a periodicity of 4 nm. The iron deposition was performed using a water-cooled e-beam evaporation cell loaded with a 99.95% pure Fe rod. The evaporation rate was calibrated through a water-cooled thickness monitor. At the typical Fe evaporation rates of $0.5\,\text{ML min}^{-1}$, the vacuum never exceeded 5×10^{-10} mbar. In our calibration, one iron monolayer is $2.1\,\text{Å}$, equivalent to the fcc iron phase layer deposited on Cu(111). Several replica samples were grown following the optimized protocol, with reproducible results for both structural and magnetic properties.

The ferromagnetic properties of the films were ascertained using *in situ* polar, longitudinal and transversal magneto-optical Kerr effect (MOKE) measurements. Each MOKE geometry uses a specific set of coils present in the preparation chamber. The coil set for longitudinal and transversal MOKE can apply a maximum magnetic field of 50 Oe, and the coil for the polar MOKE, which has an ARMCO core, can apply a magnetic field up to 1 kOe. MOKE measurements for different iron film thicknesses were measured on wedge samples that were also grown *in situ* by a moveable mask interposed between the sample surface and the e-beam source operating at a constant deposition rate of $0.5\,\text{ML min}^{-1}$, yielding a linear increase of iron thickness along the surface [11−3] direction (from 0.5 ML up to 3 ML in 5 mm).

Sample synthesis and the spectroscopic measurements were all carried out, *in situ*, at the APE-INFM beamline at the Elettra storage ring laboratory in Trieste [22]. The sample
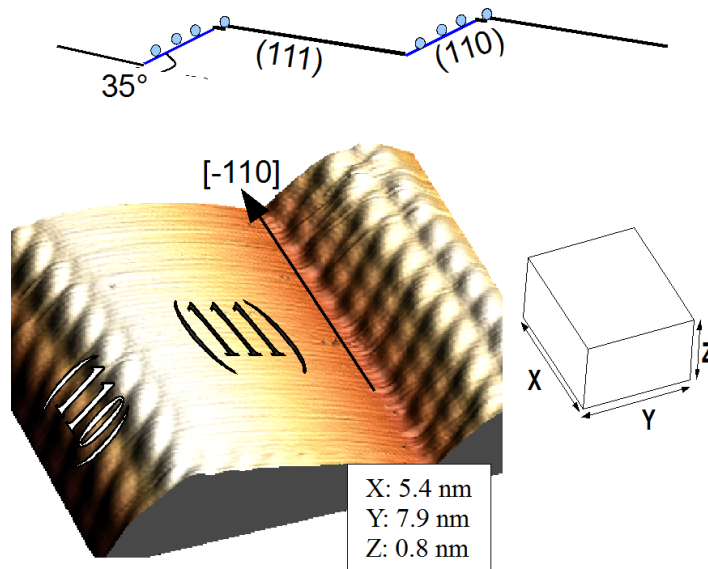
Figure 1. STM image of the oxygen-induced faceting of the Cu(332) surface. The reconstruction, consisting of alternating clean (111) facets and oxidized (110) facets, is depicted by the upper sketch in the upper panel, where the blue circles represent the oxygen atoms. The topographic image of the real surface by STM, shown in the lower panel, has been acquired with a bias voltage of -1.4 V. The feature observed on the (110) facets is ascribed to the O–Cu chains, as in the Cu(110)O(2 × 1) reconstruction.

topography was acquired at RT by operating the STM in a constant current mode with an electron-etched tungsten tip. The sample bias was set from -1.0 to -1.4 V, so as to image the occupied states. The high-resolution angle-resolved photoelectron spectroscopy (ARPES) was carried out using linearly polarized light with p-polarization from the APE low-energy branch. The spectra were measured with a SES2002 electron energy analyser operated to yield a total energy resolution (photon and analyser) of 15 meV. The spectra are therefore dominated by thermal broadening when measured at 80 K. Atom-resolved magnetometry on iron was performed by x-ray absorption circular dichroism, always *in situ*, by exploiting the radiation from the APE high-energy branch that delivers circularly polarized photons (75% in third harmonic). The energy resolution of XAS/XMCD is 200 meV at the iron edge. The beam impinges on the surface with an angle of 45° with respect to the normal and within the scattering plane formed by the surface normal and $[-110]$ vectors, and the magnetic field was applied perpendicularly to the sample surface. The XMCD at the Fe-$L_{2,3}$ edge was measured by inverting the direction of the applied magnetic field and acquiring the drain current of the sample (electron-yield mode).

3. Results and discussion

The characterization of the template substrate as well as of the iron nanowires required the concurrent use of several spectroscopic, diffractive and microscopic measurements. The topography of the substrate was investigated by STM, operated in the atomic resolution mode, at RT. The surface long-range order was checked by LEED, and the composition by AES and
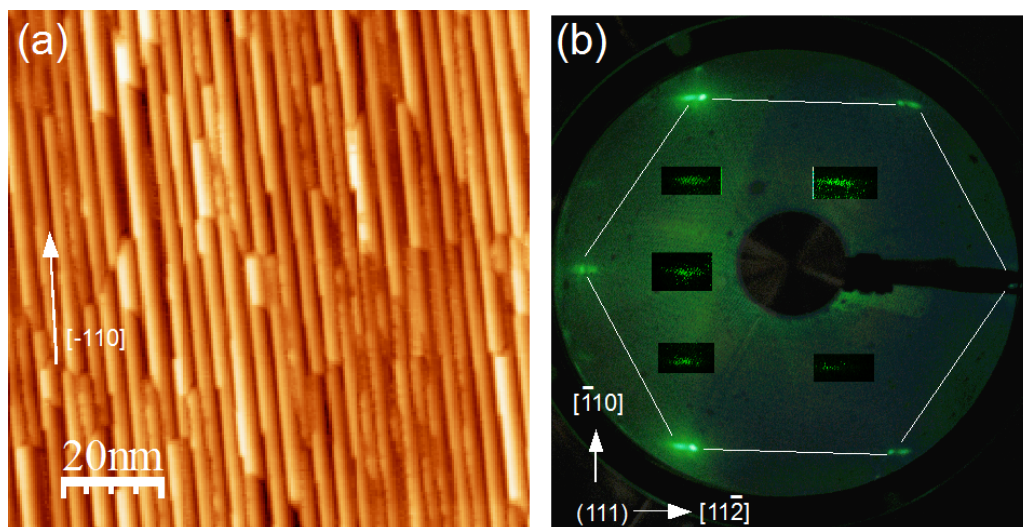
Figure 2. Oxygen-induced reconstruction of Cu(332). (a) An STM topographic image shows a striped structure with 38 Å periodicity. (b) A LEED image for the O/Cu(332); the hexagonal dashed line depicts the pattern of the (111) terrace. Note that the split along the [112] reflects the periodicity in this direction. The set of spots in the centre, where the contrast was locally enhanced, forms the rectangular pattern originated by the (2×1) superstructure on the Cu(110) facet. The electron energy is 70 eV.

core level photoemission. The surface electron states were probed by ARPES, with particular emphasis on the L-gap surface state of the Cu(111) islands that are highly sensitive to adsorbates or contamination. The magnetic order was probed by MOKE and XMCD.

Figure 2 shows the STM image of the oxidized sample (a) and its LEED pattern (b); the average periodicity is 38 Å. The LEED pattern presents a hexagonal pattern, originated from the (111) terraces, together with a rectangular pattern, attributed to the (110) facets. The splitting distance of the hexagonal pattern is about one third of the splitting in the LEED of the clean Cu(332) (not shown). The periodicity measured by LEED in the direction perpendicular to the stripes is about 36 Å, close to the value measured by the STM.

Figure 3 shows high-resolution STM images of the oxidized surface before and after Fe deposition, performed at RT (panels a and b, respectively). The striped structure of the O/Cu(332) consists of alternating (111) and oxidized (110) facets; the (110) facet can be recognized by the presence of the fringes originated by the (2×1) reconstruction in that facet. After deposition of 0.35 ML of iron, the (111) terraces are still flat while the (110) facets present a different morphology. The features highlighted by the arrows in figure 3(b) correspond to the formation of 'Cu holes' with 1 ML of height (also present for higher coverages). This process is frequently observed when an iron cluster forms near the step edges in vicinal Cu(111) [23]: the tensile stress caused by the iron nanostructures reduces the binding energy of the top atoms of the (111) terrace, allowing mass transport from the eroded parts. The flatness of the Cu(111) terraces did not significantly change after the submonolayer Fe growth, supporting the idea that (a) Fe adsorption is favoured on (110) facets and (b) Fe is responsible for the observed change of morphology. The (110) facets surface corresponds to approximately 29% of the total surface.
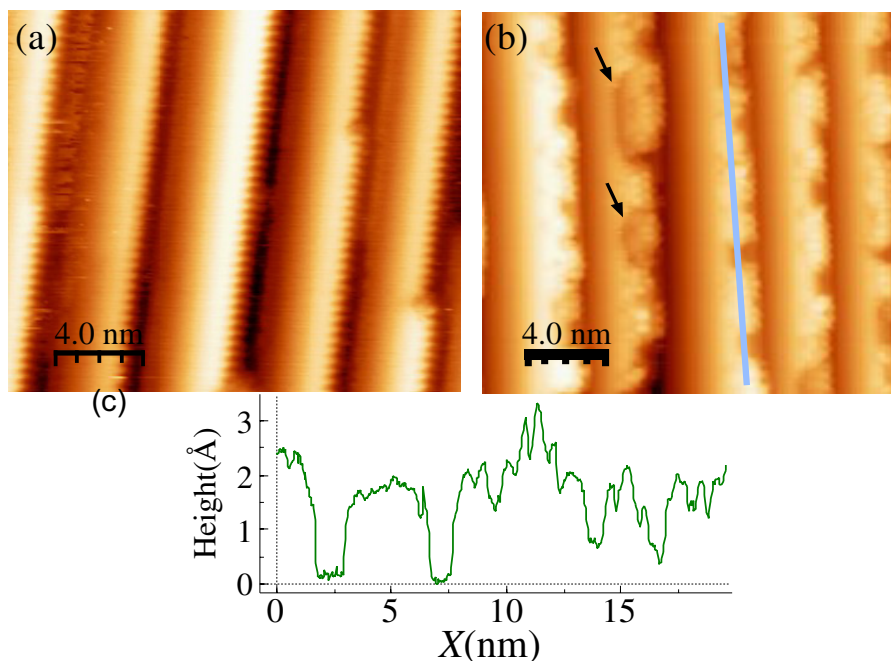
Figure 3. STM images of O/Cu(332) before (a) and after (b) iron deposition. In (a), the striped structure of the O/Cu(332) consisting of alternating (111) and oxidized (110) facets is clearly revealed; the (110) facet can be recognized by the presence of the fringes originated by the (2×1) reconstruction, as in figure 1. In (b), we see the coverage of 0.35 ML Fe on the O/Cu(332). The arrows indicate 1 ML holes on the (111) terraces. The line scan profile on the (110) facet along the $[-110]$ direction is shown in (c); see the text.

Assuming a unitary sticking coefficient and considering that the all adsorbate concentrates on the (110) facets, the deposition of 0.35 ML of Fe, evaluated for a flat surface, is equivalent to 1 ML Fe thickness on the (110) facet. In fact, the line profile (figure 3(c)), along the (110) facets, shows a quasi-continuous film with the height of approximately 2 A, suggesting a coverage close to 1 ML of iron.

The preferential growth of Fe on (110) facets was also explored by ARPES. The Cu(111) stripes of the oxidized Cu(332) template have been extensively studied by us [20] by means of ARPES, with particular attention to the dispersion characteristics of the L-gap surface state and its anisotropy due to anisotropic quantum confinement. In the present case, the relevant observation is that the L-gap surface state, which resides on the (111) terraces, is not suppressed by the deposition of iron, which corroborates the assumption of preferential adsorption on the (110) facets. Figure 4 reports the evidence that the deposition of 0.3 of Fe does not suppress the copper L-gap surface state. The surface state is still visible up to 0.7 ML of Fe thickness.

Isolated wires were obtained by depositing up to 1 ML of iron on the substrate kept at $0\,^\circ$C and using a deposition rate of $0.5\,\mathrm{ML\,min}^{-1}$ (figure 5(a)). Above that coverage, the iron incorporated on (110) moves towards the lower (111) terrace, as one can see in the 3D rendered image in panel a. The close-up of a terrace shows the atomically clean copper surface. At a coverage of 1.5 ML, we observe a modification of the morphology as shown in figure 5(b): the iron appears to cover both the (110) facet and the (111) terraces.
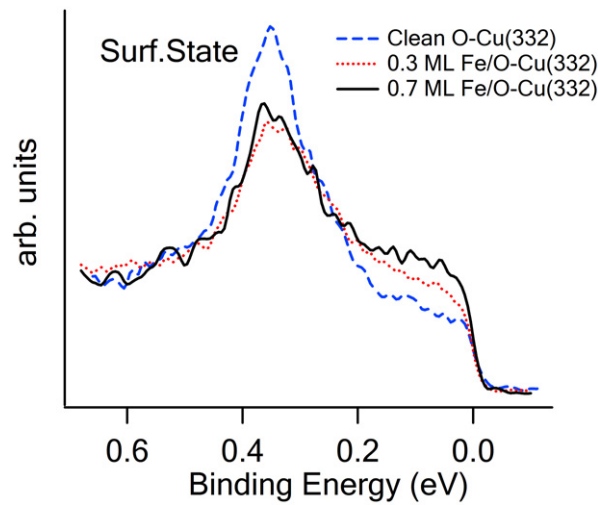
Figure 4. Photoemission of O/Cu(332) and 0.3 ML Fe/OCu(332). The surface state peak is present in both spectra. The spectra were acquired at 80 K with a photon energy of 36 eV.
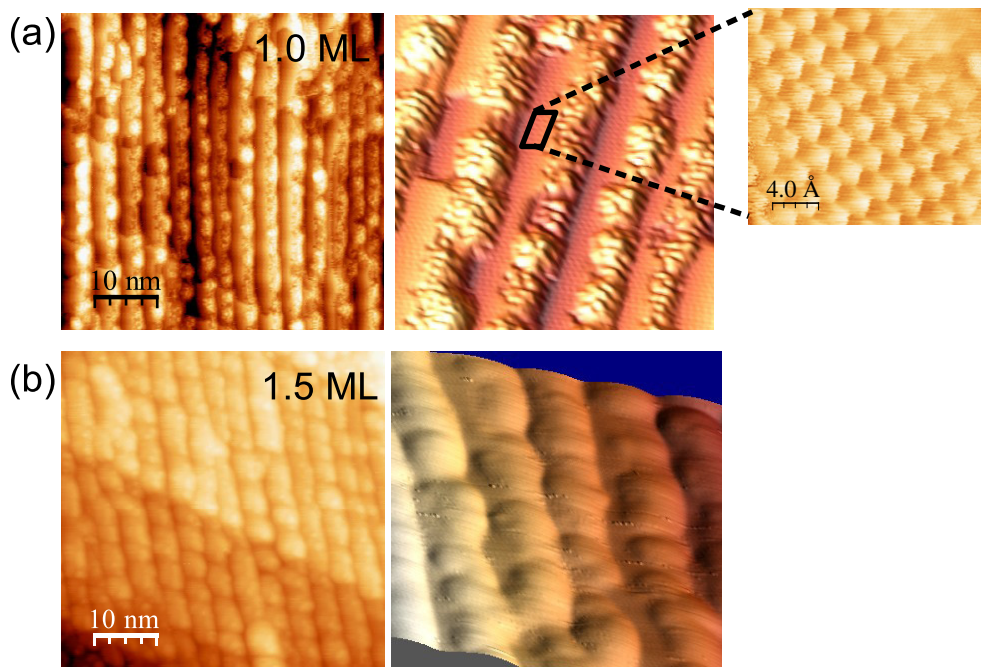

Figure 5. STM images for 1.0 ML (a) and 1.5 ML (b). In (a), the 3D rendering of the STM image shows isolated wires, while in (b) the wires appear to merge together. The inset image (15 × 15 A) in (a) shows the atomic resolution detail of the (111) terrace.

Ultrathin and quasi-1D atomic arrays of transition metals have been found to display large magnetocrystalline anisotropy [9, 26]. This is a consequence of the orbital moment being unquenched with respect to the solid state in 3D. Higher magnetic anisotropy is sought in order
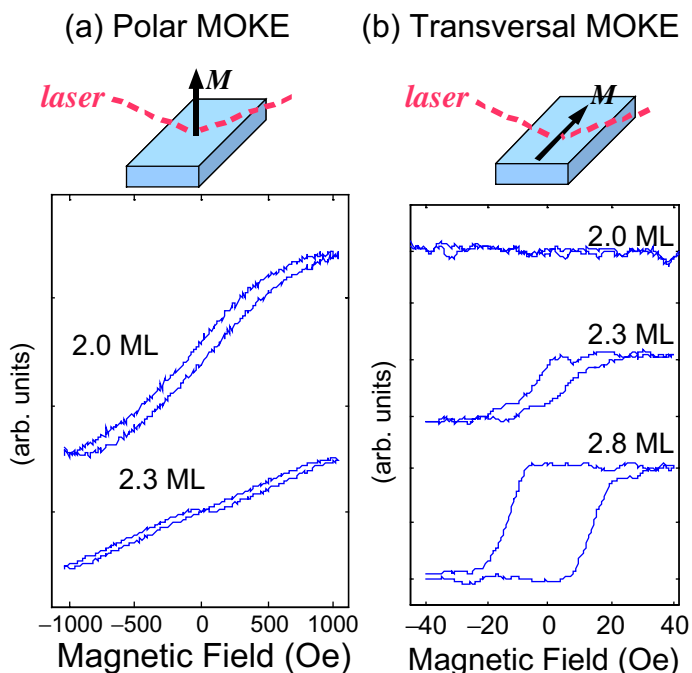
Figure 6. MOKE measurement of Fe/OCu(332) at 200 K. The magnetic fields are oriented in the [332] and [11−3] (perpendicular to the stripes), respectively, for the polar and transversal MOKE.

to push the superparamagnetic limit to smaller cluster dimensions and to exploit nanometric magnetic bits for recording purposes. It is therefore relevant to characterize the iron wires both from the point of view of a long-range magnetic order, by MOKE, and from the point of view of atomic magnetization, by XMCD. Longitudinal MOKE, i.e. with the applied H field along the stripes, gave no magnetic response at 200 K for any of the explored coverages. Polar and transversal MOKE signals are collected in figure 6 showing the Fe thickness dependence in the wedge sample. At low coverages, the perpendicular anisotropy points out of the surface plane, with a rather high coercivity. This is reduced at 2.3 ML and at higher coverages where the perpendicular anisotropy of the wires turns in-plane and the hysteresis becomes rectangular with a much reduced coercivity.

XMCD measurements were performed on a replica wedge sample (0.5–3.5 ML) at 40 K by using a oscillating pulsed magnetic field of 100 Oe along the [332] direction (out-of-plane). A typical absorption spectrum is shown in figure 7, where we compare the spectrum before and after the air exposure. Here, we stress that the XAS lineshape of iron does not show features that could be attributed to oxidized iron. The iron wires appear to be atomically pure in spite of being adsorbed on the oxidized Cu(110) facets.

The results from magnetic dichroism are presented in figure 8. The spectra of the left panel define the spectroscopic feature (magnitude of dichroism at the L_3 edge $\Delta L_3 = L_3^+ - L_3^-$) that can be taken as a measure proportional to magnetization of the iron atoms [23, 24]. The right panel of figure 8 shows the evolution of the ΔL_3 value as a function of iron thickness. For a thickness higher than 1.8 ML, one observes the decrease of the perpendicular magnetization which is consistent with a reorientation transition, or with a change from 1D isolated wires to
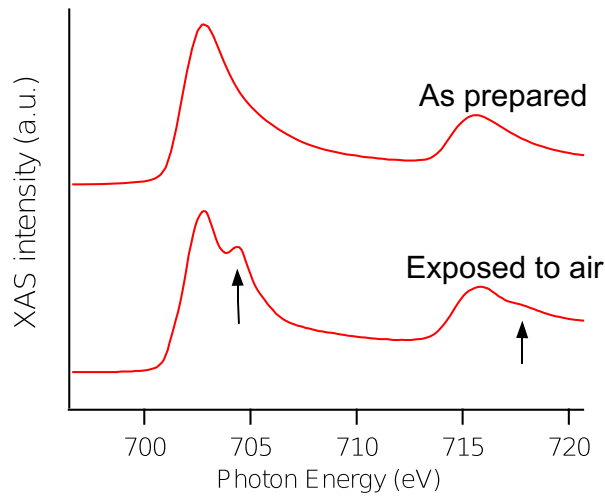
Figure 7. X-ray absorption (XAS) for 0.5 ML Fe on O-CU(332) before (top curve) and after (bottom curve) the exposure to the air. The arrows point to the peaks derived from the iron oxide.
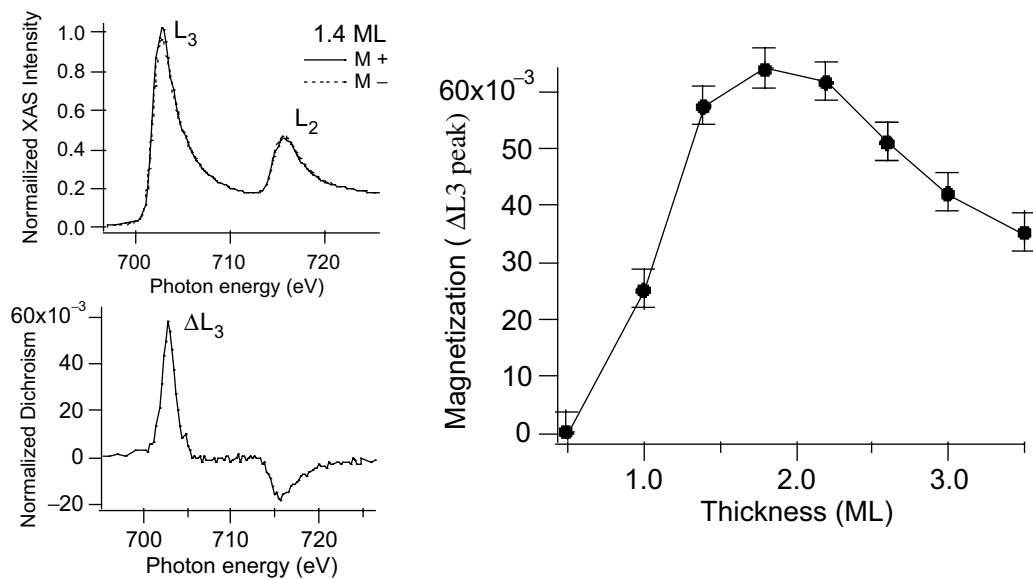

Figure 8. XMCD measurement of Fe/OCu(332). ΔL_3 versus thickness: the ΔL_3 peak intensity is *proportional to the sample magnetization* [25, 26].

a semicontinuous 2D structure. The observed transition of the easy axis occurs at a coverage when in 2D iron films on copper, the pseudomorphic fcc-like structure converts into the stable bcc one. Nevertheless, the rotation transition could be in fact due to the magnetic percolation between the wires due to the iron growth also on top of the (111) stripes, welding a corrugated 2D iron. The rectangular hysteresis loops with a low coercive field in figure 6(b) may support this picture.

4. Conclusions

Metastable nanowire growth can be easily obtained in the case of Fe/O–Cu(332) thanks to the relatively higher affinity of iron with the Cu(110)O(2 × 1) facet versus the (111) terraces. The wires are isolated for very low coverages and do display high magnetic perpendicular anisotropy. The Cu(111) stripes in between the wires are unaffected by the presence of the iron 1D network. At higher coverages, the magnetization rotates in-plane, always perpendicular to the wire direction. The present results confirm the possibility of selective growth of a quasi-1D structure on faceted surfaces when the facets present a different chemical environment to the adsorbate.

References

[1] Negulyaev N N, Stepanyuk V S, Hergert W, Bruno P and Kirschner J 2008 *Phys. Rev.* B **77** 085430
[2] Barth J V, Costantini G and Kern K 2005 *Nature* **437** 671
[3] Rohart S, Baudot G, Repain V, Girard Y, Rousset S, Bulou H, Goyhenex C and Proville L 2004 *Surf. Sci.* **559** 47
[4] Shiraki S, Fujisawa H, Nantoh M and Kawai M 2004 *Phys. Rev. Lett.* **92** 096102-1
[5] Gambardella P, Blanc M, Bürgi L, Kuhnke K and Kern K 2000 *Surf. Sci.* **449** 93
[6] Gambardella P and Kern K 2001 *Surf. Sci.* **475** L229
[7] Gambardella P 2003 *J. Phys.: Condens. Matter* **15** S2533–46
[8] Guo J, Mo Y, Kaxiras E, Zhang Z and Weitering H H 2006 *Phys. Rev.* B **73** 193405
[9] Shen J, Pierce J P, Plummer E W and Kirschner J 2003 *J. Phys.: Condens. Matter* **15** R1–30
[10] Figuera J de la, Huerta-Garnica M A, Prieto J E, Ocal C and Miranda R 1995 *Appl. Phys. Lett.* **66** 1006
[11] Pedersen M, Bonicke I A, Laegsgaard E, Stensgaard I, Besenbacher F, Ruban A and Norskov J K 1997 *Surf. Sci.* **387** 86
[12] Annese E, Viol C E, Zhou B, Fujii J, Vobornik I, Baldacchini C, Betti M G and Rossi G 2007 *Surf. Sci.* **601** 4242
[13] Bachmann A R, Speller S, Mugarza A and Ortega J E 2003 *Surf. Sci.* **526** L143
[14] Moruzzi V L, Markus P M and Kubler J 1989 *Phys. Rev.* B **39** 6957
[15] Macedo W A, Sirotti F, Panaccione G, Schatz A, Keune W, Rodrigues W N and Rossi G 1988 *Phys. Rev.* B **58** 11534
[16] Biedermann A, Rupp W, Schmid M and Varga P 2006 *Phys. Rev.* B **73** 165418
[17] Gambardela P, Dallmeyer A, Maiti K, Malagoli M C, Eberhardt W, Kern K and Carbone C 2002 *Nature* **416** 301
[18] Vindigni A, Rettori A, Pini M G, Carbone C and Gambardella P 2006 *Appl. Phys.* A **82** 385
[19] Vollmer S, Birkner A, Lukas S, Witte G and Wöll C 2000 *Appl. Phys. Lett.* **76** 2686
[20] ViolBarbosa C E and Fujii J 2008 private communication
[21] ViolBarbosa C E, Fujii J, Panaccione G and Rossi G 2009 *Surf. Sci.* **603** 3081
[22] Panaccione G *et al* 2009 *Rev. Sci. Instrum.* **80** 043105
[23] Klaua M, Höche H, Jenniches H, Barthel J and Kischner J 1997 *Surf. Sci.* **381** 106
[24] O'Brien W and Tonner B P 1994 *Phys. Rev.* B **50** 12672
[25] Chen C T, Idzerda Y U, Lin H J, Smith N V, Meigs G, Chaban E, Ho G H, Pellegrin E and Sette F 1995 *Phys. Rev. Lett.* **75** 152
[26] Sekiba D, Moroni R, Gonella G, Buatier de Mongeot F, Boragno C, Mattera L and Valbusa U 2004 *Appl. Phys. Lett.* **84** 762